Prediction of Intradialytic Hypotension Using Photoplethysmography

Kristian Solem*, Bo Olde, and Leif Sörnmo, *Senior Member, IEEE*

***Abstract*—Intradialytic hypotension is the most common acute complication during conventional hemodialysis treatment. Prediction of such events is highly desirable in clinical routine for prevention. This paper presents a novel prediction method of acute symptomatic hypotension in which the photoplethysmographic signal is analyzed with respect to changes in amplitude, reflecting vasoconstriction, and cardiac output. The method is based on a statistical model in which the noise is assumed to have Laplacian amplitude distribution. The performance is evaluated on 11 hypotension-prone patients who underwent hemodialysis treatment, resulting in seven events with acute symptomatic hypotension and 17 without. The photoplethysmographic signal was continuously acquired during treatment as was information on blood pressure and oxygen saturation. Using leave-one-out cross validation, the proposed method predicted six out of seven hypotensive events, while producing 1 false prediction out of 17 possible. The performance was achieved when the prediction threshold was chosen to be in the range 57%–65% of the photoplethysmographic envelope at treatment onset.**

***Index Terms*—Hemodialysis, intradialytic hypotension, pulse oximetry, signal processing, vasoconstriction.**

I. Introduction

DIALYSIS-INDUCED hypotension continues to be a major complication in patients with end-stage renal disease undergoing hemodialysis, despite considerable effort to shed light on its underlying cause. Hypotension not only causes discomfort to the patient, but also may increase mortality [1]–[3]. Since intradialytic hypotension leads to increased need for medical service and higher costs, it is highly desirable to develop clinical methods that helps prevent such events. It is absolutely crucial that these methods are based on sensor technology, which can be worn throughout treatment without causing discomfort to the patient. Although the mean arterial pressure may predict hypotension [4], [5], the use of a system for arterial blood pressure monitoring, such as the Finapres, is unsuitable as it is much too expensive and causes discomfort.

Manuscript received August 6, 2009; revised October 27, 2009 and December 21, 2009; accepted December 26, 2009. Date of publication February 18, 2010; date of current version June 16, 2010. This work was supported in part by grants from Gambro AB, Lund, Sweden and the Swedish Research Council. *Asterisk indicates corresponding author.*

*K. Solem was with the Department of Electrical and Information Technology, Lund University, Lund SE-220 00, Sweden. He is now with Gambro Lundia AB, Lund SE-220 10, Sweden (e-mail: kristian.solem@gambro.com).

B. Olde is with Gambro Lundia AB, Lund SE-220 10, Sweden (e-mail: bo.olde@gambro.com).

L. Sörnmo is with the Department of Electrical and Information Technology and the Center of Integrative Electrocardiology, Lund University, Lund SE-221 00, Sweden (e-mail: leif.sornmo@eit.lth.se).

Digital Object Identifier 10.1109/TBME.2010.2042170

The etiology of dialysis-induced hypotension is often considered to be volume depletion, originating from an ultrafiltration rate that exceeds the reabsorption rate. Volume depletion causes a reduction in the blood volume, which returns to the heart, resulting in decreased cardiac filling and thus decreased cardiac output that may lead to hypotension. Besides hypovolemia, other factors also contribute to intradialytic hypotension of which failing compensatory mechanisms are often considered, e.g., reflected by the autonomic nervous system (ANS), cardiac output, and capillary vasoconstriction. The analysis of heart rate variability (HRV) has primarily been employed to assess ANS activity, but has also shed light on intradialytic hypotension [6]–[10]. Although such analysis has been found useful for determining hypotension-prone patients, it has not solved the actual prediction problem. A solution to this problem may be based on the analysis of cardiac output and capillary vasoconstriction as both these factors reflect compensatory mechanisms that most likely are involved with intradialytic hypotension. Decreased cardiac output decreases the amount of blood that reaches the capillaries and, consequently, the pulse magnitude, observed in the extremities, decreases. Capillary vasoconstriction is an important autonomic counterregulating mechanism that increases blood pressure and thereby helps prevent hypotension. The blood volume in the capillaries decreases during vasoconstriction, causing a decreased pulse magnitude. Thus, both cardiac output and capillary vasoconstriction may contribute to a decreased pulse magnitude in the capillaries before hypotension occurs.

Photoplethysmography (PPG) is an optical technique for measuring blood volume changes in the microvascular bed of the tissue. The PPG technique, having found widespread clinical applications, is used to measure cardiac output and vasoconstriction as well as oxygen saturation, blood pressure, and autonomic function [11]. The interaction of light with arterial blood generates a pulsatile response due to changes in blood volume with each heartbeat, while the interaction with skin, bone, and venous blood is more constant. Therefore, the PPG signal comprises a pulsatile ("ac") component, synchronized to each heartbeat, which is superimposed on a slowly varying ("dc") baseline, related to the average blood volume and tissue properties. The baseline varies slowly due to the influence of respiration, sympathetic activity, and thermoregulation. It is well known that sympathetic activity increasingly produces vasoconstriction, which in the PPG signal is reflected by a decreased signal amplitude [12], [13].

An estimate of stroke volume may be obtained from pulse shape analysis of the PPG signal on a beat-to-beat basis, where cardiac output equals stroke volume multiplied by heart rate. Shape-related information in the PPG waveform has shown

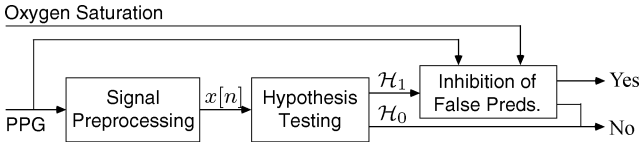

Fig. 1. Block diagram of the method for prediction of acute symptomatic hypotension. The input signals are produced by a pulse oximeter. Hypotension is predicted when the output is "Yes."

potential for assessing vasoconstriction and vasodilatation effects and may be quantified with the PPG pulse amplitude [11], [14]. This amplitude also correlates well with temperature variations since, e.g., cold exposure causes the amplitude to decrease due to vasoconstriction.

A common cause of death in renal patients is sudden cardiac death, coronary artery disease being the predominant cause [15]. Renal disease and diabetes mellitus may accelerate arteriosclerosis and arterial stiffness, which both are associated with increased risk of coronary artery disease, stroke, and heart disease. Arteriosclerosis and arterial stiffness may be detected with PPG measurements. The pulse transit time (PTT), calculated as the time difference between the ECG R-wave to the onset of the PPG pulse, decreases due to arterial stiffness since the pulse wave velocity increases. The PTT technique estimates blood pressure indirectly since arterial compliance is reduced as blood pressure increases, and the pulse wave travels faster. Ahlström *et al.* used PTT to track beat-to-beat changes in blood pressure during hemodialysis [16], but the technique was not applied to the prediction of hypotension.

Over the last few decades, pulse oximetry represents a significant technological advance in clinical monitoring [18]. A pulse oximeter uses PPG measurements in order to obtain information about arterial blood oxygen saturation and heart rate [19]. Oxygen saturation is determined from the PPG dc component and the corresponding amplitude ratio of the red and near infrared ac component, whereas heart rate is determined from the ac component. Venous oxygen saturation as an estimate of cardiac output was recently suggested for prediction of hypotension during hemodialysis [20]. Arterial oxygen saturation was also studied for this purpose, investigating changes in the variance of the saturation signal as predictor information [21].

In this study, pulse oximetry is the starting point for developing a novel approach to the prediction of acute symptomatic, intradialytic hypotension. The method employs the normalized envelope of the PPG signal, measured at the finger, as an indirect measure of cardiac output and capillary vasoconstriction. The predictor is based on statistical detection theory, employing a model of the PPG signal in which the noise is assumed to be Laplacian. To the best of our knowledge, the PPG signal has never before been considered for prediction of hypotension. The different processing blocks that define the present method are displayed in Fig. 1.

II. Methods

A. Signal Preprocessing

The PPG signal is first subjected to high-pass filtering for the purpose of baseline wander removal as implemented by the following procedure. Since the acquisition device implements autoscaling (see shortly), low frequency information can be removed without causing problems. An estimate of the baseline wander is obtained by downsampling the PPG signal to 2 Hz, followed by forward/backward filtering, using a second-order low-pass Butterworth filter with a cutoff frequency of 0.5 Hz. The low-pass-filtered signal is then upsampled and subtracted from the original PPG signal, resulting in a high-pass-filtered signal denoted $p[k]$. It should be noted that the choice of cutoff frequency is not critical as subsequent signal processing does not rely on faithful pulse shape reproduction.

Changes in relative blood volume in the capillaries are assumed to be reflected by changes in the envelope of $p[k]$. A simple approach to obtaining a signal, which reflects such changes, is to compute the *normalized integrated* PPG (niPPG) signal $x[n]$, defined by

$$x[n] = \frac{1}{\bar{P}} \sum_{k=nK-L+1}^{nK} |p[k]| \tag{1}$$

where K and L are positive integers that define the downsampling step and the moving average interval, respectively. Downsampling is admissible since L is chosen so large that the smoothing of $p[k]$ transforms its pulsatile nature into a slowly changing envelope. The normalization factor $\bar{P}$ is determined as an average of the initial 5 min of the unnormalized but smoothed and rectified $p[k]$, assuming that the blood pressure remains stable during this period (which in practice is almost invariably the case).

B. Detector Structure

In this study, the essential hypothesis is that a decrease in $x[n]$ reflects capillary vasoconstriction and decreased cardiac output, here is assumed to precede hypotension. This hypothesis is translated to the problem of detecting a change in level of the niPPG signal in a window that slides as new data becomes available. The level detection problem is first treated for a fixed time window, indexed by m, in which hypothesis testing is performed; then, the resulting detector is extended to handle a sliding window.

The detection procedure is based on a model in which the level is either equal to 1 (hypothesis $\mathcal{H}_0$), or reduced to $1-\Delta A$ (hypothesis $\mathcal{H}_1$)

$$\begin{aligned} \mathcal{H}_0: &\quad x[m] = 1 + w[m], && m = 0, 1, \ldots, N-1 \\ \mathcal{H}_1: &\quad x[m] = 1 - \Delta A + w[m], && m = 0, 1, \ldots, N-1 \end{aligned} \tag{2}$$

where $x[m]$ is the observed niPPG signal, ΔA is the unknown change in level ($0 < \Delta A \leq 1$), N is the number of samples in the time window, and $w[m]$ is assumed to be independent and identically distributed zero-mean Laplacian noise with known variance σ^2. This probability density function (PDF) is assumed since outliers sometimes occur in the niPPG signal; the validity of this assumption is investigated in Section IV-A.

The level change detector is based on the Neyman–Pearson theorem in which the probability of detection P_D is maximized for a given probability of false alarm $P_F = \alpha$ by deciding $\mathcal{H}_1$

if [23]

$$L(\mathbf{x}) = \frac{p(\mathbf{x};\mathcal{H}_1)}{p(\mathbf{x};\mathcal{H}_0)} > \gamma' \tag{3}$$

where $p(\mathbf{x};\mathcal{H}_i)$ denotes the PDF of $\mathbf{x}$ under $\mathcal{H}_i$, and $\mathbf{x}$ is an $N \times 1$ vector with the observations $x[0], x[1], \ldots, x[N-1]$. The threshold γ' is determined from

$$P_F = \int_{\{\mathbf{x}:L(\mathbf{x})>\gamma'\}} p(\mathbf{x};\mathcal{H}_0)\, d\mathbf{x} = \alpha. \tag{4}$$

Since the PDF under $\mathcal{H}_1$ in (2) contains the unknown parameter ΔA, the generalized-likelihood ratio test (GLRT) is employed in which ΔA is first estimated using maximum-likelihood (ML) estimation and then inserted into $L(\mathbf{x})$ in (3) [23]. Thus, the GLRT decides $\mathcal{H}_1$ if

$$L_G(\mathbf{x}) = \frac{p(\mathbf{x};\hat{A},\mathcal{H}_1)}{p(\mathbf{x};\mathcal{H}_0)} > \gamma' \tag{5}$$

where $\hat{A}$ is the ML estimate of $A = 1 - \Delta A$ assuming that $\mathcal{H}_1$ is true (and consequently maximizes $p(\mathbf{x};A,\mathcal{H}_1)$). It is well known that the estimator of A is the median, i.e.,

$$\hat{A} = \text{median}\{x[0], x[1], \ldots, x[N-1]\}. \tag{6}$$

The PDFs in (5) are given by

$$p(\mathbf{x};\hat{A},\mathcal{H}_1) = \frac{1}{(2\sigma^2)^{\frac{N}{2}}} \exp\left[-\sqrt{\frac{2}{\sigma^2}}\sum_{m=0}^{N-1}|x[m]-\hat{A}|\right] \tag{7}$$

and

$$p(\mathbf{x};\mathcal{H}_0) = \frac{1}{(2\sigma^2)^{\frac{N}{2}}} \exp\left[-\sqrt{\frac{2}{\sigma^2}}\sum_{m=0}^{N-1}|x[m]-1|\right] \tag{8}$$

respectively. Thus, the GLRT becomes

$$L_G(\mathbf{x}) = \frac{\exp\left[-\sqrt{\frac{2}{\sigma^2}}\sum_{m=0}^{N-1}|x[m]-\hat{A}|\right]}{\exp\left[-\sqrt{\frac{2}{\sigma^2}}\sum_{m=0}^{N-1}|x[m]-1|\right]} > \gamma' \tag{9}$$

or, equivalently

$$\sqrt{\frac{\sigma^2}{2}}\ln L_G(\mathbf{x}) = -\sum_{m=0}^{N-1}\Big(|x[m]-\hat{A}| - |x[m]-1|\Big) > \sqrt{\frac{\sigma^2}{2}}\ln\gamma'. \tag{10}$$

Simplifying this expression, we obtain the following test statistic, which decides $\mathcal{H}_1$ if

$$G(\mathbf{x}) = 1 + \frac{1}{N}\sum_{m=0}^{N-1}\Big(|x[m]-\hat{A}| - |x[m]-1|\Big) < \gamma \tag{11}$$

where the threshold γ is determined by a given P_F. Thus, the optimal GLRT detector evaluates the difference between the mean deviation from $\hat{A}$ and the mean deviation from 1.

Since $0 \le \Delta A \le 1$, an alternative, attractive way of expressing $G(\mathbf{x})$ is (see the Appendix)

$$G(\mathbf{x}) = \frac{2}{N}\sum_{m=0}^{N-1}\tilde{x}[m] \tag{12}$$

where $\tilde{x}[m]$ is defined as

$$\tilde{x}[m] = \begin{cases} 0, & x[m] < \hat{A} \\ x[m], & \hat{A} < x[m] \le 1, \\ 1, & x[m] > 1 \end{cases} \qquad m = 0, \ldots, N-1. \tag{13}$$

If one or several samples $x[m]$ are equal to $\hat{A}$, some samples should be zeroed in order to assure that half of all values of $\tilde{x}[m]$ are zero. Thus, $G(\mathbf{x})$ may be viewed as the mean value of the samples $x[m]$, which exceed $\hat{A}$, with all $x[m]$'s larger than one set to one.

The test statistic $G(\mathbf{x})$ has the advantage of being limited to values between 0 and 1, and therefore $G(\mathbf{x})$ can be interpreted as an estimate of the dc level in $x[m]$. It should also be noted that the values produced by the estimator $\hat{A}$ are similar to those produced by $G(\mathbf{x})$, thus suggesting that $\hat{A}$ itself can be employed as a test statistic.

In order to track changes in A, a sliding window approach is introduced in which $G(\mathbf{x})$ is replaced with

$$G(\mathbf{x}[n]) = 1 + \frac{1}{N}\sum_{m=0}^{N-1}\Big(|x[m+n]-\hat{A}[n]| - |x[m+n]-1|\Big) < \gamma \tag{14}$$

where

$$\hat{A}[n] = \text{median}\{x[n], x[n+1], \ldots, x[n+N-1]\}. \tag{15}$$

Hypothesis $\mathcal{H}_1$ is decided when $G(\mathbf{x}[n])$ drops below γ for the first time, and thereby determines the time $\hat{n}$ that predicts hypotension. When expressed in minutes, the prediction time is given by

$$\hat{\tau} = (\hat{n} + N - 1)\cdot 60T_s \tag{16}$$

where T_s denotes the sampling interval of $x[n]$. Prediction performance is partly evaluated in terms of the difference between the true time of hypotension τ, obtained by manual annotation as described shortly, and the prediction time $\hat{\tau}$, i.e., $\Delta\tau = \tau - \hat{\tau}$, where $\Delta\tau$ denotes the time of prediction.

C. Inhibition of False Predictions

The PPG and oxygen saturation signals are subjected to special analysis for the purpose of avoiding false predictions due to saturation conditions. When a prediction occurs, its validity is first tested with respect to basic characteristics of these two signals, possibly leading to its rejection.

The pulse oximeter requires a restarting period once saturation occurs in the PPG signal, causing the ac component to disappear, see Fig. 2. As a consequence, the niPPG signal becomes zero during the restarting period and may, therefore, trigger a prediction. Such a false prediction is, however, easily eliminated when the saturation exceeds 1 s. A shorter saturation does not cause a restarting period.

When the pulse oximeter sensor comes into contact with, the niPPG and oxygen saturation signals may decrease although the PPG signal is not saturated. Thus, when the oxygen saturation is zero, a false prediction can be eliminated irrespective of the value in the PPG signal. A false prediction triggered when the

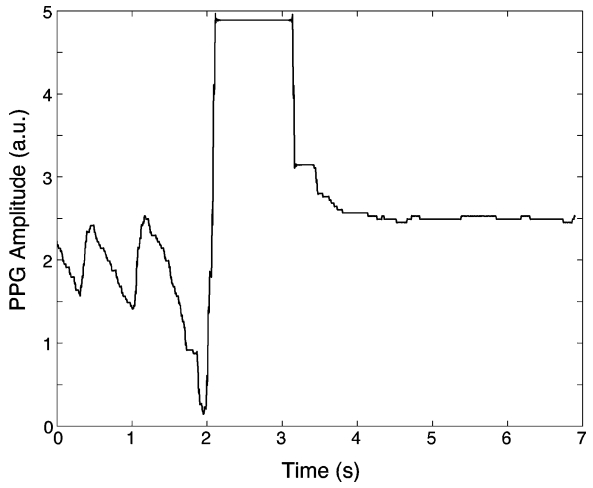

Fig. 2. PPG signal containing a saturation event with onset at about 2 s. A prediction triggered during saturation is eliminated with the present method.

finger is removed from the sensor can also be eliminated since both the PPG and oxygen saturation signals are zero.

III. Equipment and Dataset

A. Equipment

Data were acquired with a blood pressure monitor and a pulse oximeter instrument, operating in parallel with the conventional hemodialysis equipment. Two types of dialysis machines were used in this study, the Gambro AK 200 and the Gambro AK 200 Systems (Gambro Lundia AB, Sweden), on patients who underwent hemodialysis and hemodialysis filtration, respectively. The dialyzer filters were selected according to each patient's individual requirements.

A continuous arterial blood pressure signal was acquired with the Portapres (Finapres Medical Systems BV, Holland), using a Biopac MP150 data acquisition system (BIOPAC Systems, Inc., USA) at 1000-Hz sampling rate. The blood pressure was measured with two finger cuffs wrapped around the mid-phalanx of two different fingers on the hand of the access-free arm. The blood pressure was measured with one finger cuff at a time, the measurements being performed during 15 min on one cuff before the measurements were changed to the other cuff for 15 min, and so forth. The blood pressure was not measured during eating since the finger cuff was removed due to patient comfort. If the blood pressure measurements failed, they were measured manually. The blood pressure was also measured manually at the onset and end of treatment as a reference. The measurement hand was held close to the heart level during treatment. Different cuff sizes and adjacent fingers were used when inaccurate blood pressure measurements were obtained. The arterial blood pressure signal was measured for the purpose of defining the true time of symptomatic hypotension τ, as annotated by the clinical staff, and determining if the symptomatic hypotension was acute or not, see shortly.

The PPG and oxygen saturation signals were acquired continuously, using a pulse oximeter (LifeSense, Medair AB, Sweden) and the aforementioned Biopac MP150 system. The original sampling rate of 1000 Hz was decimated to 200 Hz so as to reduce oversampling. The pulse oximeter used a finger sensor, which was attached to the same hand as where the blood pressure was measured, on one of the fingers free from the blood pressure finger cuff. The sensor was attached to the finger during the entire treatment.

B. Patient Groups

Eleven patients with end-stage renal failure, who underwent regular hemodialysis treatment three times a week, participated in the study. Each treatment lasted from 3 to 5 h. A physician classified patients at the clinic as either hypotension-resistant or hypotension-prone, and only hypotension-prone patients were included. The physician's decision was based on each patient's clinical history such as the number of hypotensive events per month. The average likelihood of hypotension during treatment within the course of the last month for the 11 patients was 41%. There was a total of four male and seven female patients with an average age of 64 ± 12 years and an average weight of 70 ± 20 kg. The study, performed at Rigshospitalet, Copenhagen, Denmark, was voluntary and approved by the local ethics committee.

A total of 28 treatments were acquired from the 11 patients, although only 25 treatments were analyzed since the pulse oximeter could not be used in three treatments due to cold hands or sensor problems. There were 17 treatments without symptomatic hypotension, classified as treatments with stable blood pressure. The clinical staff identified and annotated ten symptomatic hypotensive events in eight treatments for which the patients experienced nausea, dizziness, vomiting, and fainting. These ten events were then classified offline with the help of the blood pressure signal. Seven of the ten events were classified as acutely symptomatic, here defined as a sudden drop in systolic blood pressure (30 mmHg per 10 min before hypotension [10]); these events occurred in five treatments of which two exhibited double occurrence of hypotension. The three remaining treatments were excluded since the symptomatic hypotension was due to either a gradual decrease in blood pressure over the entire treatment or a consistently low blood pressure; see Section V for comments. Thus, performance was investigated on seven events with acute symptomatic hypotension and 17 without.

IV. Results

A. Laplacian Distribution

The assumption of Laplacian noise $w[n]$ in (2) is based on the general observation that the niPPG signal sometimes contains outliers. In order to validate the feasibility of this assumption, the niPPG signals from the 17 treatments without symptomatic hypotension were analyzed. The mean value, determined for each treatment, was removed from the niPPG signal in order to produce $w[n]$. The resulting amplitude histogram of all samples is displayed in Fig. 3, indicating that $w[n]$ is largely Laplacian in nature and quite deviating from the Gaussian PDF.

The envelope of the niPPG signal is not constant during the entire treatment, but the negative tail is slightly heavier than that

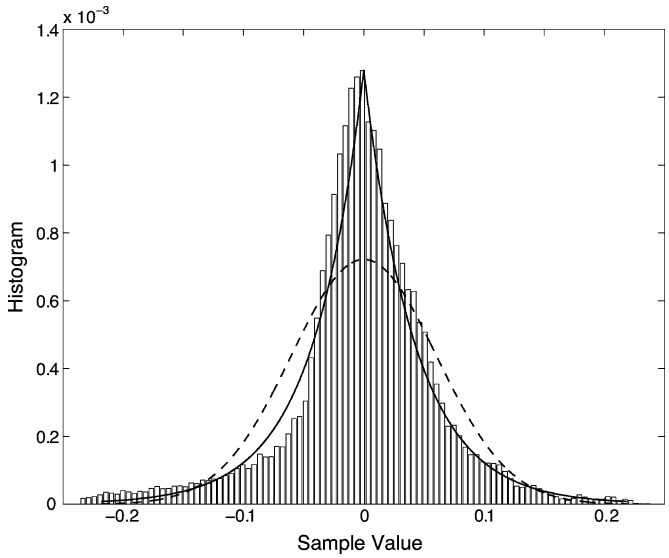

Fig. 3. Amplitude histogram of the niPPG signals obtained from patients without symptomatic hypotension. The Laplacian and Gaussian PDFs are superimposed (solid and dashed line, respectively) with the variance set to that of the observed niPPG signals.

TABLE I
NUMBER OF CORRECTLY PREDICTED ACUTE SYMPTOMATIC HYPOTENSIVE EVENTS (N_D) AND NUMBER OF FALSELY PREDICTED EVENTS (N_F)

γ	0.4	0.5	0.6	0.7
N_D (out of 7)	2	4	6	7
N_F (out of 17)	0	0	1	2

of the Laplacian model. This is due to the fact that the envelope is more likely to decrease than increase during treatment, see Fig. 3.

B. Prediction of Hypotension

The performance was studied using the following parameter values: the moving average interval L was set to 1 min, and the downsampling step K to 5 s, i.e., $L \gg K$, and the time window length N was set to 5 min. The fourth, and last, parameter that defines the method is the prediction threshold γ whose influence on performance is studied later on.

Table I presents the number of correctly predicted hypotensive events (N_D) and the number of falsely predicted events (N_F) for different values of the threshold γ when applied to the decision function $G(\mathbf{x}[n])$.

Further insight into the choice of γ was provided by employing a variation of the leave-one-out cross-validation procedure, designed to account for the fact that we are more interested in predicting all the true episodes than in minimizing the false-positive predictions. In this procedure, the training set consisted of six out of seven acute symptomatic events, whereas the evaluation set consisted of the left-out event and the 17 events without symptomatic hypotension. The procedure was repeated seven times such that all acutely symptomatic hypotensive events were once left out from the training set, and the results were then averaged. For each evaluation in the cross validation, the lowest γ-value that produced no error for the six events was first determined and then applied to the $1 + 17$ events, thus producing a range of optimal thresholds. The results are presented in Table II, showing that six out of seven left-out events were correctly predicted, and that 7 out of 119 were incorrectly predicted, i.e., 1 out of 17. The optimal thresholds were found to be in the range 0.57–0.65.

TABLE II
TOTAL NUMBER OF CORRECTLY PREDICTED ACUTE SYMPTOMATIC HYPOTENSIVE EVENTS (N_D) AND TOTAL NUMBER OF FALSELY PREDICTED EVENTS (N_F) USING A VARIATION ON LEAVE-ONE-OUT CROSS VALIDATION (SEE TEXT FOR DETAILS)

γ	0.57–0.65
N_D (out of 7)	6
N_F (out of $7 \cdot 17 = 119$)	7

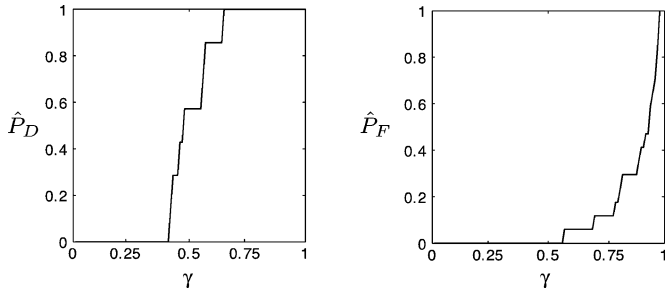

Fig. 4. Estimated probabilities $\hat{P}_D$ and $\hat{P}_F$ as a function of γ.

Taking the total number of patients with and without acute symptomatic hypotension into account (7 and 17, respectively), Fig. 4 presents estimates of the probability of correctly predicted events (P_D) and the probability of falsely predicted events (P_F), displayed as a function of γ; this diagram format is preferred over the commonly used receiver operating characteristic for reasons of legibility. It is obvious that $\hat{P}_F$ increases much more slowly than does $\hat{P}_D$ when γ increases, suggesting that there is a range of γ-values, which produce a low P_F while maintaining a high P_D.

The mean time of prediction $\overline{\Delta\tau}$ is displayed as a function of γ in Fig. 5; this quantity results from averaging of the different values of $\Delta\tau$ from the seven hypotensive treatments. For $\gamma = 0.6$, the resulting $\overline{\Delta\tau}$ was found to be 38 min.

C. Signal Examples

Fig. 6 displays blood pressure (systolic and diastolic) and $G(\mathbf{x}[n])$ during 3-h dialysis treatment of a patient without symptomatic hypotension. The dips occurring every 30 min in systolic blood pressure are due to periodic shifting of the finger cuffs used for measurement, see Section III-A.

Data from a patient with acute symptomatic hypotension are presented in Fig. 7. A marked change in level occurs in the decision function prior to the actual occurrence of hypotension. The patient is eating from 120 to 140 min (blood pressure measurement is flat during this period), and hypotension occurs just after eating is finished at 144 min. This behavior is quite common during hemodialysis, since eating causes blood to be

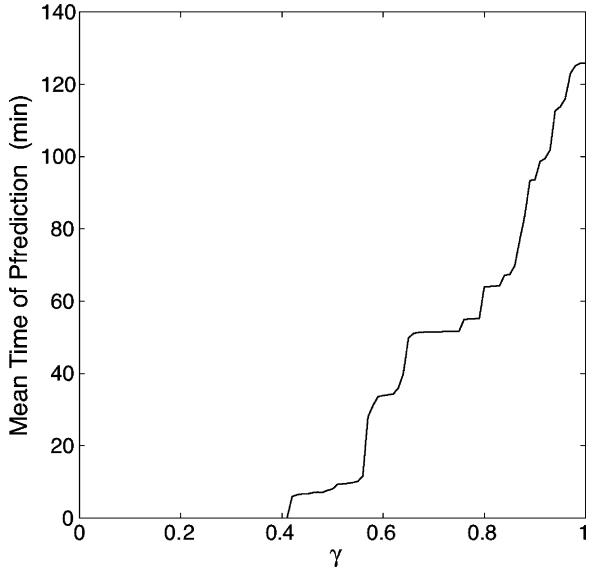

Fig. 5. Mean time of prediction $\overline{\Delta\tau}$ as a function of γ.

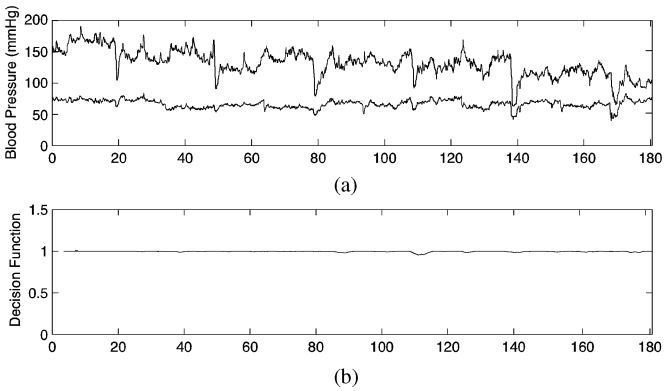

Fig. 6. Patient during hemodialysis treatment without symptomatic hypotension. (a) Systolic and diastolic blood pressure and (b) decision function $G(\mathbf{x}[n])$.

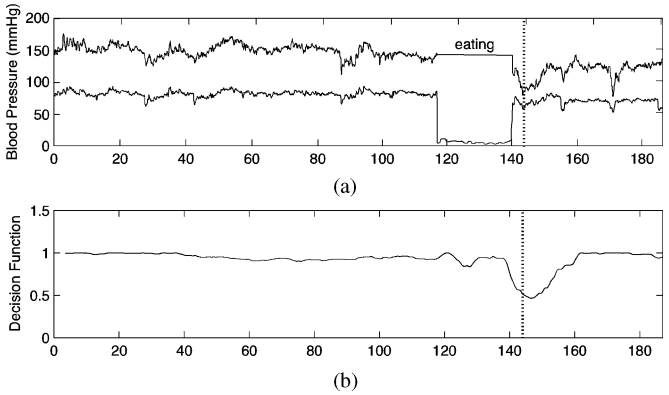

Fig. 7. Patient during hemodialysis treatment with acute symptomatic hypotension occurring at 144 min (dashed line). (a) Systolic and diastolic blood pressure and (b) decision function $G(\mathbf{x}[n])$.

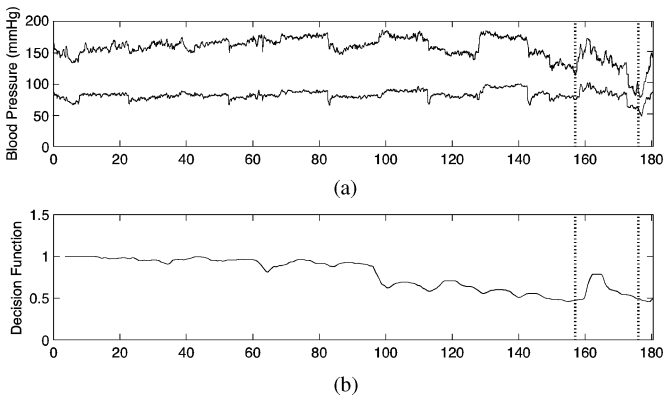

Fig. 8. Patient during hemodialysis treatment with two acute symptomatic hypotensions occurring at 157 and 176 min (dashed lines). (a) Systolic and diastolic blood pressure and (b) decision function $G(\mathbf{x}[n])$.

drawn to the stomach, which reduces the blood volume in the vascular system and causes the blood pressure to drop. Hence, hypotension was most likely induced by eating in this case.

Fig. 8 displays data from a patient with two events of acute symptomatic hypotension. A marked change takes place in the decision function prior to both events. After the first event, different interventions were carried out in order to restore blood pressure, using Trendelenburg's position, cessation of ultrafiltration, and infusion of saline bolus. As a result, $G(\mathbf{x}[n])$ increased for a short period of time.

V. Discussion

While intradialytic hypotension represents a major complication in clinical routine, very few studies have actually described methods for its prediction with performance characterized in explicit terms such as $\hat{P}_F$, $\hat{P}_D$, and $\overline{\Delta\tau}$. The present study introduces a novel approach to the prediction of hypotension, which is based on information acquired from a pulse oximeter. The method is very simple to implement in a real-time monitoring system and appears to be feasible from a clinical viewpoint since the required PPG sensor is lightweight, small sized, inexpensive, and does not impose much constraints neither on the patient nor on the medical staff during treatment.

The pulse oximeter method explores information contained in the long-term variations in the ac component of the PPG signal. This information can be extracted in various ways, e.g., by computing the envelope [25] or the peak-to-peak amplitude of successive waves. Since these two approaches either require the computation of the Hilbert transform or waveform-related processing, a simple approach was here adopted with which the desired information can still be extracted. The computation of the niPPG signal in (1) requires just additions and no multiplication in order to produce an output sample. The filter parameter L was set to 5 min in order to strike a good balance between delay and few false predictions. This choice is uncritical for the method's performance as long as it is not taken to be considerably smaller, e.g., on the order of a few seconds. If so, the niPPG signal will reflect movements and deep inspiratory gasping, which will cause false predictions [11]. It should be pointed out that no differences in performance were found when either of the three aforementioned preprocessing techniques was used.

The noise in the niPPG signal was assumed to be independent, identically distributed Laplacian. Although the real noise is more complex in nature than what can be characterized by this model, the assumption is still reasonable to pursue as the amplitude histogram is largely Laplacian, see Fig. 3. Staying away from the computational complications that come with the assumption of generalized Gaussian noise, the other feasible assumption may be that of Gaussian noise. In that case, the ML estimator of the level A is identical to computing the mean value of $x[0], \ldots, x[N-1]$ instead of the median. As one may expect, the performance of the Gaussian predictor is inferior to that of the Laplacian predictor, mostly due to that the former predictor produces more false predictions.

In a previous study, we proposed an ECG-based method for detecting intradialytic hypotension, relying information on HRV and the occurrence of ectopic beats [10]. HRV was characterized by the ratio between low- and high-frequency content, and the occurrence of ectopic beats by a running estimate of the beat count; a decrease in the ratio or an increase in ectopic beat count served as an indication of hypotension. The indicators were complementary as HRV analysis cannot be performed when several ectopic beats are present. Comparing the ECG-based method with the present pulse oximeter method, it is evident that the latter method offers the technical advantage of providing a decision function being defined for all time instants. Although a running estimate of the beat count can be computed for all time instants, its accuracy is highly dependent on the actual number of ectopic beats that occur; this number may differ quite considerably from one patient to another. Other factors that speak in favor of the present method is the extra time needed to attach the ECG electrodes and the inconvenience to carry them, and the much more demanding set of signal processing algorithms, which is required for ECG analysis.

In a recent study, short-term variability of oxygen saturation was suggested as a "warning parameter" of intradialytic hypotension, quantified by the running standard deviation [21]. It was hypothesized that increased variability precedes hypotension, being a consequence of various changes in cardiac output and tissue perfusion. Using a threshold of 0.85, 17 out of 20 treatments with hypotension were correctly predicted and 18 out of 20 treatments without hypotension; the mean time of prediction was 14 min. In contrast to the present study, information on the true time of hypotension τ was made use of when determining $\hat{\tau}$, thereby making a comparison of results difficult. The oxygen saturation method in [21] could not be applied to the present dataset due to differences in the measurement of oxygen saturation.

The PPG signal is sensitive to various types of artifacts. Touching the sensor or moving the sensor hand are two common situations during dialysis treatment, which introduce artifacts in the niPPG signal. Large artifacts are also introduced in the niPPG signal when a patient is coughing. During treatment it is customary to measure manual blood pressure with a cuff strapped around the upper arm. Such a measurement is always performed on the same arm as the pulse oximeter measurements, since it is inappropriate to measure blood pressure on the access arm. The niPPG signal will be zero during a blood pressure measurement, since the cuff around the arm ceases all blood volume variations to the fingers. Substantial efforts have recently gone into the development of signal processing techniques for improving the immunity to artifacts when analyzing the PPG signal, see, e.g., [26], [27]. Still, additional algorithms that are tailored to the dialysis situation may be warranted to ensure robust performance.

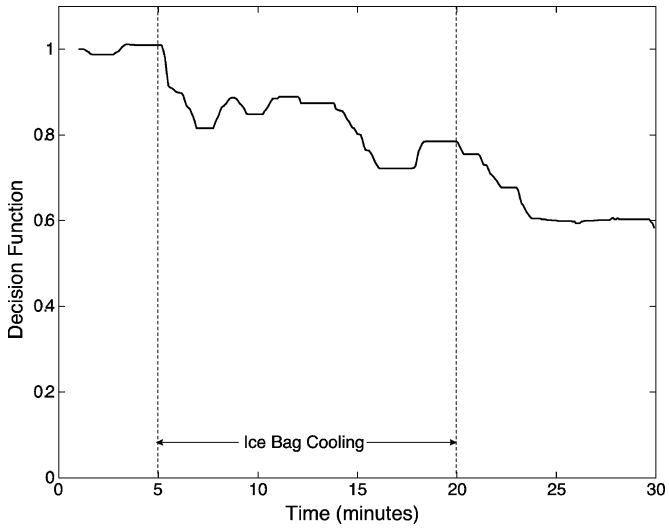

Fig. 9. Decision function $G(\mathbf{x}[n])$ during cooling of a hand with the sensor positioned on the index finger. Cooling started after 5 min by putting an ice bag around the hand and ended after 20 min. The hand was still cold at the end of the recording.

Different techniques for prediction of symptomatic hypotension, using mean arterial pressure in combination with linear extrapolation, may be successfully applied to the three symptomatic hypotension treatments (see Section III-B) with a gradual decrease in blood pressure or consistently low blood pressure. However, such techniques will most likely experience difficulties when producing an early prediction of the seven events of acute symptomatic hypotension since these events are unexpected. The present study is focused on the prediction of the latter type of event.

The niPPG signal is influenced by temperature changes such that cold fingers will lead to capillary vasoconstriction and, consequently, the niPPG signal will decrease. Fig. 9 illustrates this property for a hand, which was cooled during 15 min with a bag of ice; the pulse oximeter sensor was attached to the hand.

A limitation with the present study is that the dataset is too small for making far-reaching conclusions about the overall value of the pulse oximeter method; more data are obviously needed to do this. Still, the results suggest that the method has great potential and, as determined by the leave-one-out cross-validation procedure, the choice of the threshold value γ was not particularly critical as the suitable range was found to be 0.57–0.65.

It should be emphasized that the present dataset is not representative of the average dialysis patient, but of patients, which are hypotension prone. A hypotension-resistant patient is considered to have a more intact ANS than a hypotension-prone patient [10], [24]. Thus, the niPPG signal would better reflect

cardiac output and capillary vasoconstriction in a resistant patient than in one, which is prone.

VI. Conclusion

A novel method for the prediction of acute symptomatic hypotension during hemodialysis is developed, which is based on information derived from pulse oximetry. A decrease in the envelope of the PPG signal, assumed to reflect capillary vasoconstriction and a decrease in cardiac output, serves as the predictive information. The method is simple in structure and involves very few design parameters, and is therefore suitable not only for clinical dialysis treatment but also in home dialysis treatment. The resulting prediction performance are promising as six out of seven events with acute intradialytic hypotension could be predicted, whereas only 1 false prediction out of 17 possible was produced. However, these results are preliminary and a larger dataset needs to be studied in order to establish the overall value of the present method.

Appendix

In order to obtain the ML estimator of the level $A = 1 - \Delta A$ in (2), denoted $\hat{A}$, the PDF of $\mathbf{x}$, defined by

$$p(\mathbf{x}; A) = \frac{1}{(2\sigma^2)^{\frac{N}{2}}} \exp\left[-\sqrt{\frac{2}{\sigma^2}} \sum_{n=0}^{N-1} |x[n] - A|\right] \tag{17}$$

needs to be maximized over A. This maximization is equivalent to minimize the cost function

$$J(A) = \sum_{n=0}^{N-1} |x[n] - A| \tag{18}$$

with respect to A. If the samples $x[0], x[1], \ldots, x[N-1]$ are excluded from the differentiation, since $J(A)$ is a discontinuous function at these points, we obtain

$$\frac{dJ(A)}{dA} = -\sum_{n=0}^{N-1} \operatorname{sgn}(x[n] - A) \tag{19}$$

where $\operatorname{sgn}(x[n] - A) = 1$ if $A < x[n]$ and $\operatorname{sgn}(x[n] - A) = -1$ if $A > x[n]$, which is set to zero if A is chosen as the median of $x[0], x[1], \ldots, x[N-1]$.

From $G(\mathbf{x})$ in (11), we have

$$\begin{aligned} G(\mathbf{x}) &= 1 + \frac{1}{N} \sum_{n=0}^{N-1} (|x[n] - \hat{A}| - |x[n] - 1|) \\ &= 1 + \frac{1}{N} \left[\sum_{x[n]<\hat{A}} (\hat{A} - x[n]) + \sum_{x[n]>\hat{A}} (x[n] - \hat{A}) \right. \\ &\qquad \left. - \sum_{x[n]<1} (1 - x[n]) - \sum_{x[n]>1} (x[n] - 1) \right]. \end{aligned} \tag{20}$$

Since $0 \le \Delta A \le 1$, i.e., $\hat{A} \le 1$, we have

$$\begin{aligned} G(\mathbf{x}) &= 1 + \frac{1}{N} \left[\sum_{x[n]>\hat{A}} x[n] - \sum_{x[n]<\hat{A}} x[n] - \sum_{x[n]<\hat{A}} 1 \right. \\ &\qquad + \sum_{x[n]<\hat{A}} x[n] - \sum_{\hat{A}<x[n]<1} 1 + \sum_{\hat{A}<x[n]<1} x[n] \\ &\qquad \left. - \sum_{x[n]>1} x[n] + \sum_{x[n]>1} 1 \right] \\ &= 1 + \frac{1}{N} \left[2 \sum_{\hat{A}<x[n]<1} x[n] - N_{\hat{A}<x[n]<1} + N_{x[n]>1} \right. \\ &\qquad \left. - N_{x[n]<\hat{A}} \right] \end{aligned} \tag{21}$$

where $N_{\hat{A}<x[n]<1}$ is the number of $x[n]$ in the interval $\hat{A} < x[n] < 1$; $N_{x[n]>1}$ and $N_{x[n]<\hat{A}}$ are defined in the same way. Note that $N_{x[n]<\hat{A}} = N_{x[n]>\hat{A}}$. Thus,

$$\begin{aligned} G(\mathbf{x}) &= 1 + \frac{1}{N} \left[2 \sum_{\hat{A}<x[n]<1} x[n] - 2N_{\hat{A}<x[n]<1} \right] \\ &= \frac{2}{N} \sum_{n=0}^{N-1} \tilde{x}[n] \end{aligned} \tag{22}$$

where $\tilde{x}[n]$ is defined as

$$\tilde{x}[n] = \begin{cases} 0, & x[n] < \hat{A} \\ x[n], & \hat{A} < x[n] \le 1, \\ 1, & x[n] > 1 \end{cases} \qquad n = 0, 1, \ldots, N-1. \tag{23}$$

Acknowledgment

The authors would like to thank Dr. Ladefoged and Dr. Cordtz at the Department of Nephrology, Rigshospitalet, Copenhagen, Denmark, for their strong support during data acquisition.

References

[1] J. T. Daugirdas, "Dialysis hypotension: A hemodynamic analysis," *Kidney Int.*, vol. 39, pp. 233–246, 1991.

[2] S. Cavalcanti, A. Ciandrini, S. Severi, F. Badiali, S. Bini, A. Gattiani, L. Cagnoli, and A. Santoro, "Model-based study of the effects of the hemodialysis technique on the compensatory response to hypovolemia," *Kidney Int.*, vol. 65, pp. 1499–1510, 2004.

[3] T. Shoji, Y. Tsubakihara, M. Fujii, and E. Imai, "Hemodialysis-associated hypotension as an independent risk factor for two-year mortality in hemodialysis patients," *Kidney Int.*, vol. 66, pp. 1212–1220, 2004.

[4] X. Chen, D. Xu, G. Zhang, and R. Mukkamala, "Forecasting acute hypotensive episodes in intensive care patients based on a peripheral arterial blood pressure waveform," in *Proc. Comput. Cardiol.*, 2009, vol. 36, pp. 545–548.

[5] P. Langley, S. King, D. Zheng, E. J. Bowers, K. Wang, J. Allen, and A. Murray, "Predicting acute hypotensive episodes from mean arterial pressure," in *Proc. Comput. Cardiol.*, 2009, vol. 36, pp. 553–556.

[6] M. G. W. Barnas, W. H. Boer, and H. A. Koomans, "Hemodynamic patterns and spectral analysis of heart rate variability during dialysis hypotension," *J. Amer. Soc. Nephrol.*, vol. 10, pp. 2577–2584, 1999.

[7] B. Fahn, G. Wirnsberger, H. Hutten, and H. Holzer, "Intradialytic heart rate variability in hypotension-prone and hypotension-resistant hemodialysis patients," *J. Amer. Soc. Nephrol*, vol. 11, p. 265A, 2000.
[8] S. Cavalcanti, S. Severi, and G. Enzmann, "Analysis of oscillatory components of short-term heart rate variability in hemodynamically stable and unstable patients during hemodialysis," *Artif. Organs*, vol. 22, pp. 98–106, 1998.
[9] G. Pelosi, M. Emdin, C. Carpeggiani, M. A. Morales, M. Piacenti, P. Dattolo, T. Cerrai, A. Macerata, A. L'Abbate, and Q. Maggiore, "Impaired sympathetic response before intradialytic hypotension: A study based on spectral analysis of heart rate and pressure variability," *Clin. Sci.*, vol. 96, pp. 23–31, 1999.
[10] K. Solem, A. Nilsson, and L. Sörnmo, "An electrocardiogram-based method for early detection of abrupt changes in blood pressure during hemodialysis," *ASAIO J.*, vol. 52, pp. 282–290, 2006.
[11] J. Allen, "Photoplethysmography and its application in clinical physiological measurement," *Physiol. Meas.*, vol. 28, pp. R1–R39, 2007.
[12] M. Nitzan, A. Babchenko, B. Khanokh, and D. Landau, "The variability of the photoplethysmographic signal. A potential method for the evaluation of the autonomic nervous system," *Physiol. Meas.*, vol. 19, pp. 93–102, 1998.
[13] R. P. Schnall, A. Shlitner, J. Sheffy, R. Kedar, and P. Lavie, "Periodic, profound peripheral vasoconstriction: A new marker of obstructive sleep apnea," *Sleep*, vol. 22, pp. 939–946, 1999.
[14] E. D. Cooke, S. A. Bowcock, and A. T. Smith, "Photoplethysmography of the distal pulp in the assessment of the vasospastic hand," *Angiology*, vol. 36, no. 1, pp. 33–40, 1985.
[15] R. Ranpuria, M. Hall, C. T. Chan, and M. Unruh, "Heart rate variability (HRV) in kidney failure: Measurement and consequences of reduced HRV," *Nephrol. Dial. Transplant.*, vol. 23, pp. 444–449, 2008.
[16] C. Ahlström, A. Johansson, F. Uhlin, T. Länne, and P. Ask, "Noninvasive investigation of blood pressure changes using the pulse wave transit time: A novel approach in the monitoring of hemodialysis patients," *J. Artif. Organs*, vol. 8, pp. 192–197, 2005.
[17] B. P. M. Imholz, W. Wieling, G. A. van Montfrans, and K. H. Wesseling, "Fifteen years experience with finger arterial pressure monitoring: Assessment of the technology," *Cardiovasc. Res.*, vol. 38, no. 3, pp. 605–616, 1998.
[18] J. G. Webster, *Design of Pulse Oximeters*. Bristol, U.K.: Institute of Physics Publishing, 1997.
[19] I. Yoshiya, Y. Shimada, and K. Tanaka, "Spectrophotometric monitoring of arterial oxygen saturation in the fingertip," *Med. Biol. Eng. Comput.*, vol. 18, pp. 27–32, 1980.
[20] J. Cordtz, B. Olde, K. Solem, and S. Ladefoged, "Central venous oxygen saturation and thoracic admittance during dialysis: New approaches to hemodynamic monitoring," *Hemodial. Int.*, vol. 12, pp. 369–377, 2008.
[21] E. Mancini, L. Corazza, M. L. Soverini, D. C. Cannarile, S. Cavalcanti, S. Cavani, A. Fiorenzi, and A. Santoro, "Short-term variability of oxygen saturation during hemodialysis is a warning parameter for hypotension appearance," in *Proc. Comput. Cardiol.*, 2008, vol. 35, pp. 881–883.
[22] L. Sörnmo and P. Laguna, *Bioelectrical Signal Processing in Cardiac and Neurological Applications*. Amsterdam, The Netherlands: Elsevier, 2005.
[23] S. M. Kay, *Fundamentals of Statistical Signal Processing, Vol. II: Detection Theory*. Upper Saddle River, NJ: Prentice-Hall, 1998.
[24] K. Solem, P. Laguna, J. P. Martínez, and L. Sörnmo, "Model-based detection of heart rate turbulence," *IEEE Trans. Biomed. Eng.*, vol. 55, no. 12, pp. 2712–2722, Dec. 2008.
[25] E. Gil, J. Maria Vergara, and P. Laguna, "Detection of decreases in the amplitude fluctuation of pulse photoplethysmography signal as indication of obstructive sleep apnea syndrome in children," *Biomed. Signal Process. Control*, vol. 3, pp. 267–277, 2008.
[26] S. H. Kim, D. W. Ryoo, and C. Bae, "Adaptive noise cancellation using accelerometers for the PPG signal from forehead," in *Proc. IEEE Conf. Eng. Med. Biol. Soc.*, 2007, pp. 2564–2567.
[27] L. B. Wood and H. H. Asada, "Low variance adaptive filter for cancelling motion artifact in wearable photoplethysmogram sensor signals," in *Proc. IEEE Conf. Eng. Med. Biol. Soc.*, 2007, pp. 652–655.

Kristian Solem received the M.Sc. degree in electrical engineering and the Ph.D. degree in biomedical signal processing from Lund University, Lund, Sweden, in 2003 and 2008, respectively.

He is currently with the Research Department, Gambro Lundia AB, Lund, Sweden. His research interests include ECG, pressure, and photoplethysmography signals and their significance in heart-rate variability analysis, heart-rate turbulence analysis, and hemodialysis.

Bo Olde received the M.Sc. degree in engineering of applied physics and the Ph.D. degree in applied electronics from Lund University, Lund, Sweden, in 1982 and 1991, respectively.

He is currently a Principal Scientist at the Research Department, Gambro Lundia AB, Lund, Sweden. His research interests include clinical research in the field of hemodialysis.

Leif Sörnmo (S'80–M'85–SM'02) received the M.Sc. and Ph.D. degrees in electrical engineering from Lund University, Lund, Sweden, in 1978 and 1984, respectively.

From 1983 to 1995, he was a Research Fellow at the Department of Clinical Physiology, Lund University, where he was engaged in research on ECG signal processing. Since 1990, he has been with the Signal Processing Group, Department of Electrical and Information Technology, Lund University, where he is currently a Professor of biomedical signal processing. He is the author or coauthor of *Bioelectrical Signal Processing in Cardiac and Neurological Applications* (Elsevier, 2005). His main research interests include statistical signal processing, modeling of biomedical signals, methods for atrial fibrillation analysis, multimodal signal processing in hemodialysis, detection of otoacoustic emissions, and power-efficient signal processing in implantable devices.

Dr. Sörnmo is an Associate Editor of the IEEE TRANSACTIONS ON BIOMEDICAL ENGINEERING and the *Journal of Electrocardiology*, a member of the Editorial Board of the *Medical and Biological Engineering and Computing*, and has been an Associate Editor of the *Computers in Biomedical Research* (1997–2000).